IEEE Transactions on Nuclear Science, Vol. NS-27, No. 3, June 1980

# SPECT: SINGLE PHOTON EMISSION COMPUTED TOMOGRAPHY

Ronald J. Jaszczak
R. Edward Coleman
*Chun Bin Lim

P. O. Box 3949
Duke University Medical Center
Durham, North Carolina 27710

## Summary

Interest in single photon emission computed tomography (SPECT) has been renewed as a result of the successful application of transmission (x-ray) CT to diagnostic radiology. Many aspects of SPECT are different from those encountered in transmission CT, and often are more difficult to overcome. Examples of two major aspects encountered are 1) the limitations on the available photon flux imposed mainly by dose considerations to the patient and, 2) the internal attenuation of gamma rays within the patient prior to detection. Progress has been made recently in overcoming the quantum limitation by designing SPECT systems using special collimation and large active detector areas. High efficiency systems have been designed and built using both multiple-scanners and also using multiple large-field-of-view scintillation cameras. Much progress has also been made in compensating for the problem of gamma ray attenuation using iterative and analytical approaches. This paper reviews the history of single photon emission tomography, characterizes the physical attributes of SPECT, describes some solutions to the inherent problems encountered, and also reviews a few selected approaches in designing SPECT systems to provide high quality, artifact-free reconstructed images. It is anticipated that future developments will allow SPECT systems to more nearly attain the ultimate goal of determining absolute regional radionuclide concentration as a function of time. These systems, coupled with newly developed physiological radiopharmaceuticals, can provide useful research and clinical information.

## Introduction

Transmission computed tomography (TCT) using x-rays has had a major impact on diagnostic medicine since its clinical introduction by EMI, Ltd. in 1971.[1,2,3,4] As a result of this impact the inventor of the clinical system, Godfrey Hounsfield, shared the 1979 Nobel Prize for Physiology and Medicine with Allan Cormack, who independently implemented a solution in 1963 to the reconstruction problem.[5,6,7].

The concept of transverse section imaging using a transmission source was first introduced by Oldendorf in 1961[8] Later, in the 1970's the groups consisting of Berry and Gibbs,[9] Shepp and Logan,[10] Herman et al[11] and Bates and coworkers[12,13,14] presented solutions to the x-ray reconstruction problem based on Fourier techniques. An iterative approach to the x-ray problem was developed by Goitein in 1972.[15] It is interesting to note that a solution to the general mathematical problem of CT had been previously proposed by Radon in 1917.[16]

*Current address: EMI Medical, Inc.
4000 Commercial Avenue
Northbrook, Illinois 60062

As might be expected a retrospective analysis indicates that the problem of reconstructing a two-dimensional function from a set of line integrals measured at various angles has applications in many diverse fields of endeavor besides the obviously significant one of diagnostic radiology using x-rays. For example during the period when Cormack and Hounsfield were developing their solutions, Bracewell et al (1954-1967) were solving the "strip integration" problem as it relates to the reconstruction of two-dimensional brightness distributions in radio astronomy.[17,18,19,20] De Rosier and coworkers,[21,22] Ramachandran and Lakshminarayanan[23] and Gordon et al[24] investigated similar reconstruction problems in the field of electron microscopy.

Historically, emission transverse section tomography using single photon emission sources was first introduced by Kuhl and Edwards in 1963.[25] Their devices detected gamma rays emitted along lines in a section by using alternate translation and angular indexing motions.

Thus, their instrument was the first single photon emission tomograph. Their original algorithms were based on simple backprojection techniques[25,26,27,28,29] and were implemented both optically and digitally. Later algorithms were developed by Kuhl et al using more accurate interative solutions for digital computer processing.[30,31,32,33] Kuhl et al had also investigated the utility of transmission transverse tomography using simple backprojection as early as 1966.[34]

The scanner based approach developed by Kuhl has subsequently been investigated by Bowley et al,[35] Keyes et al,[36] Myers et al[37] and Patton et al.[38,39] Single photon transverse section tomography using a camera based approach was first investigated by Anger et al[40,41] and Harper et al.[42,43] Scintillation camera based SPECT systems have been investigated by Bellini et al,[44] Budinger et al,[45,46,47] Jaszczak et al,[48,49,50,51,52] Kay et al,[53] Keyes et al,[54] Oppenheim et al[55,56] and Muehllehner et al.[57,58]

Emission computed tomography in nuclear medicine has developed in two complementary directions; detection of annihilation coincidence radiation from positron emitters, and detection of single photon radiation. Positron ECT (sometimes referred to as PET) systems have the advantage of using physiologically important radionuclides such as $^{11}C$, $^{13}N$, $^{15}O$, and $^{18}F$; however most positron radionuclides presently can only be produced with an expensive and complex on-site particle accelerator. Single photon emission computed tomography (SPECT) has the practical advantage of using

0018-9499/80/0600-1137$00.75©1980 IEEE

readily available radiopharmaceuticals; however, these radiopharmaceuticals are less physiologically significant. This paper is limited in scope to a review of single photon emission tomography with particular emphasis on its physical rather than clinical characteristics. General emission tomography reviews have previously been presented (for example, see Phelps[59] and Budinger et al[60]).

## Radionuclide Imaging

A concentration C( $\mu$ Ci/ $cm^3$) of a radionuclide in an organ occurs following the internal administration of a selected radiopharmaceutical. The spatial and temporal distribution of this concentration function within an organ can provide important information concerning organ function and pathology. The goal of emission computed tomography is to determine the absolute radionuclide regional concentration as a function of time. This goal is quite difficult to accomplish in practice; however, often relative regional concentrations obtained after equilibrium (thereby eliminating the temporal dependency) can provide useful functional information. Many SPECT systems currently being investigated are directed toward this less ambitious objective. It is anticipated that the quantitative aspects will have increased importance as these systems are improved and new radiopharmaceuticals are developed. Kuhl et al have already demonstrated that SPECT can provide absolute concentration measurements in certain imaging situations.[31,32,33]

Emission CT differs from transmission CT in that emission CT attempts to measure a physiological parameter, namely the uptake (or lack of uptake) of a radiopharmaceutical tracer within the body; whereas, transmission or x-ray CT generally attempts to measure a physical parameter, namely the attenuation coefficient. Of course, if an x-ray contrast agent is used, then a physiological measurement can be made with the transmission CT system. These latter systems require good statistical measurements because 1) the object contrast is inherently low since the difference between attenuation coefficients for abnormal and normal tissue is generally quite small (one or two percent) and, 2) the high spatial resolution demands precise input data.

In nuclear medicine, the target-to-nontarget concentration ratio R is typically quite large. For example, R might be as much as ten or twenty for lesions in the brain. It is the specificity of radiopharmaceuticals which allows radionuclide images to provide useful diagnostic information even though the measured data is of poor statistical quality. In SPECT imaging, as in conventional radionuclide imaging, a trade-off can be made between system sensitivity and system resolution. Other aspects of the measurement process are described in the following sections.

## Detection Systems

Diagnostic nuclear medicine and SPECT depend upon the collimation of emitted gamma rays prior to interaction within the detector in obtaining a projection view of the radionuclide distribution. Currently conventional nuclear medicine systems use a NaI(Tl) scintillation crystal as the gamma ray detector. The first gamma ray imaging devices developed by Cassen et al[61,62] in the late 1940's and early 1950's consisted of a scintillation detector mechanically scanned in a rectilinear raster above the unknown source distribution (Fig. 1-A). The relative intensity of detected gamma rays is mapped as a function of scanner position to generate an image of the radionuclide distribution. The gamma ray detection efficiency of such systems is limited because of the inherent sequential nature of the photon detection process.

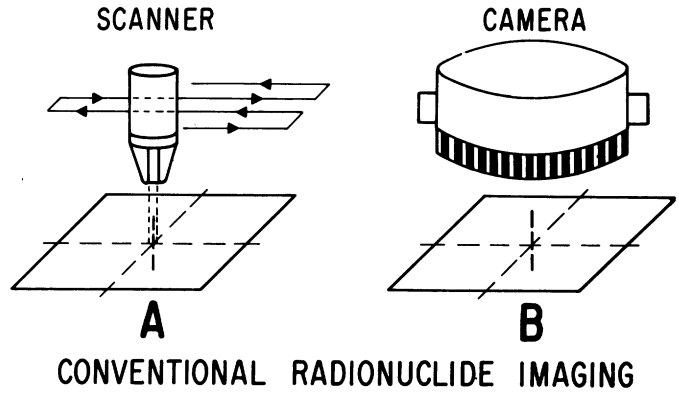


Figure 1. Basic nuclear medicine imaging geometries.

Two events have dramatically influenced the course of nuclear medicine imaging. The first event was the invention of the scintillation camera (Figs. 1-B and 2) by Anger[63,64] in 1957. Instead of a mechanical scanning approach, the Anger camera is based on the use of a stationary single, large diameter scintillation crystal viewed by an array of photomultiplier tubes. Analog circuitry is used to determine the location of a gamma ray interaction within the crystal. Thus, the whole organ may be viewed at one time. The other significant event was the development of the Tc-99m (140 keV) generator by Harper et al in 1962.[65,66] Having a physical half-life of six hours, this radionuclide is well suited for routine clinical use, and the Anger scintillation camera tended to be optimized for these 140 keV photons. Today most nuclear medicine imaging is performed using scintillation cameras based on the Anger principal.

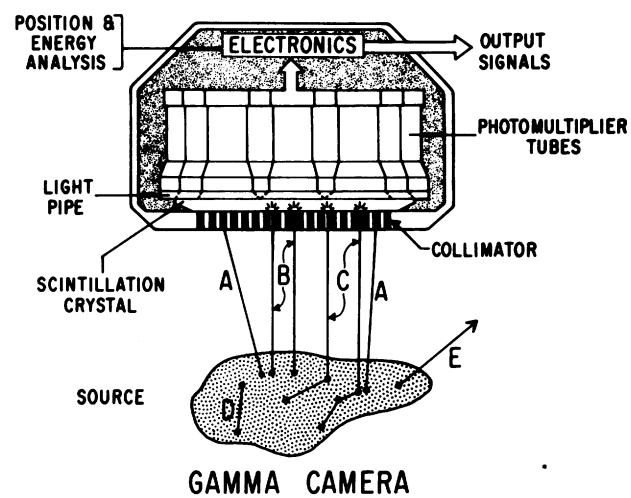


Figure 2. Scintillation camera. Several possible gamma ray interactions that can occur within the source, collimator and crystal are illustrated.

## SPECT Measurement Process

Both scanner based and camera based detector systems have been adapted to generate high quality SPECT images. Before proceeding to descriptions of specific implementations it is useful to briefly review

the interaction of the emitted gamma rays within the patient and the detection system. Figure 2 schematically illustrates a scintillation camera viewing an internal gamma ray source embedded within the body of the patient. It can be noted that this situation is quite different from that of transmission x-ray CT where an external source is used. Since the gamma ray source is contained within a three-dimensional volume, and emits isotropically, detectors with a large active surface area should be used. Ideally 4 $\pi$ solid angle detection would be optimal. As a result of practical (economical) limitations, a choice must usually be made when designing SPECT systems whether to have higher sensitivity for a single slice (scanner based approaches), or to have lower sensitivity per slice but higher overall sensitivity by viewing the entire organ simultaneously (camera based approaches). In any event the efficiency is mainly determined by the detection solid angle, which is typically proportional to the useful detector area.

Other differences between emission and transmission CT are illustrated in Figure 2. Two important interactions of gamma rays and matter are Compton scattering (event C) and internal attenuation (event D). Simple reconstruction algorithms use the assumption that the projection data corresponds to line integrals of the photon emission density along each ray for all angular samples. The effect of attenuation results in a decrease in the actual line integral measured as compared with the value one would obtain if there were no attenuation. For 140 keV gamma rays, approximately one-half are stopped in 5 cm of water (equivalent to soft tissue). Thus, this effect can not be ignored. The magnitude of the attenuation depends upon the gamma ray energy and the composition of the attenuating medium (being different, for example, for soft tissue, bone, and lungs). Ideally it would be desirable to correct for nonuniform attenuation; however, reasonably adequate results have been obtained for most imaging situations by assuming a constant attenuation coefficient, i.e., a homogeneous attenuating medium of known dimensions.

Another aspect of emission CT is the inclusion in the line integral of gamma rays internally scattered within the patient. At a photon energy of 140 keV, the most probable interaction of gamma rays within the body is the Compton scattering process. Gamma rays may also undergo Compton scattering within the detector (not shown in Figure 2) and then escape; however, this effect is less probable with NaI(Tl) than with solid state detectors such as germanium (Ge). The effect of Compton scatter on SPECT imaging is described in a later section.

In the next section we review the basic geometries currently being used in emission tomography. A review of the backprojection process and solutions to the practical problems encountered in implementing a SPECT system are then presented.

## Geometries for Radionuclide Emission Tomography

Radionuclide emission tomographic systems may be classified by several different methods. For example, one might classify the devices according to the type of detector used, i.e. scanner based or camera based. In this manuscript two basic geometries are described. If the primary reconstruction is performed for planes (or sections) parallel to the long axis of the body, the emission tomographs are described as longitudinal section imaging systems (Fig. 3). If the primary reconstruction is performed for planes perpendicular to the body axis, the term transverse section imaging is used to described the systems (Fig. 4).

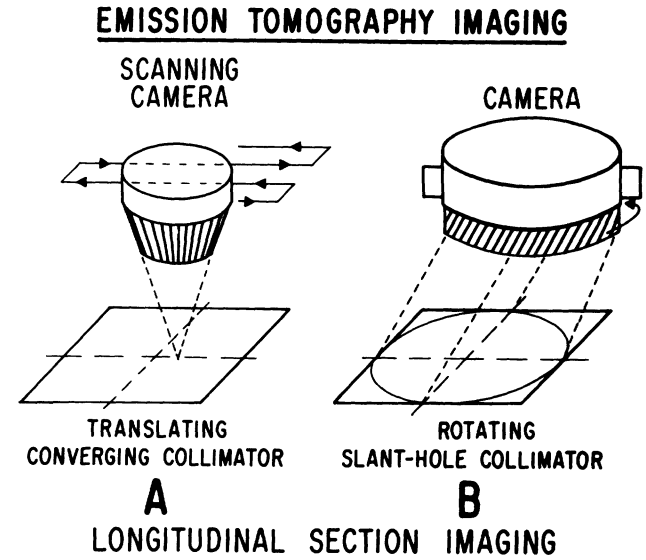


Figure 3. Focal-plane or incomplete angular sampling emission tomography.

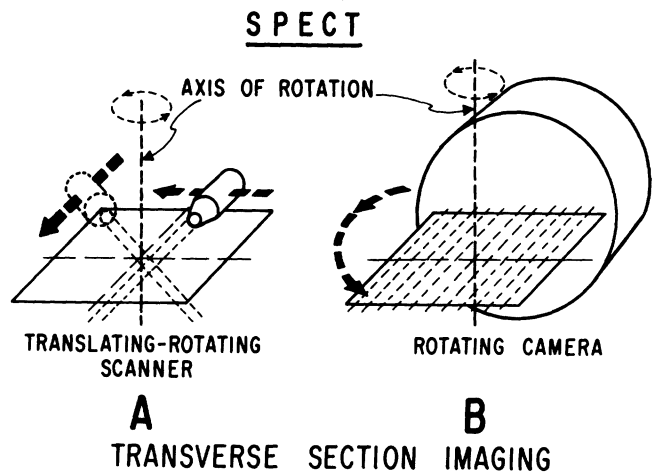


Figure 4. Complete angular sampling approaches to single photon emission computed tomography (SPECT).

It must be noted that this division of approaches is somewhat arbitrary since systems have been implemented which allow both geometries to be used. Furthermore, by using a data reorganization algorithm it is possible to obtain a set of longitudinal sections from a complete set of contiguous transverse sections. The argument for using this classification is related to the elimination of overlying and underlying sources of activity. In general, longitudinal section systems collect data from different sections in a coupled manner. In transverse section imaging this coupling is removed by treating the 3-D volume as a stack of 2-D sections during the data collection process. Thus, transverse section imaging systems can collect a complete set of angular samples from individual sections by scanning about the axis of rotation. Activity along the axis of rotation is isolated into separate transverse planes by using collimation.

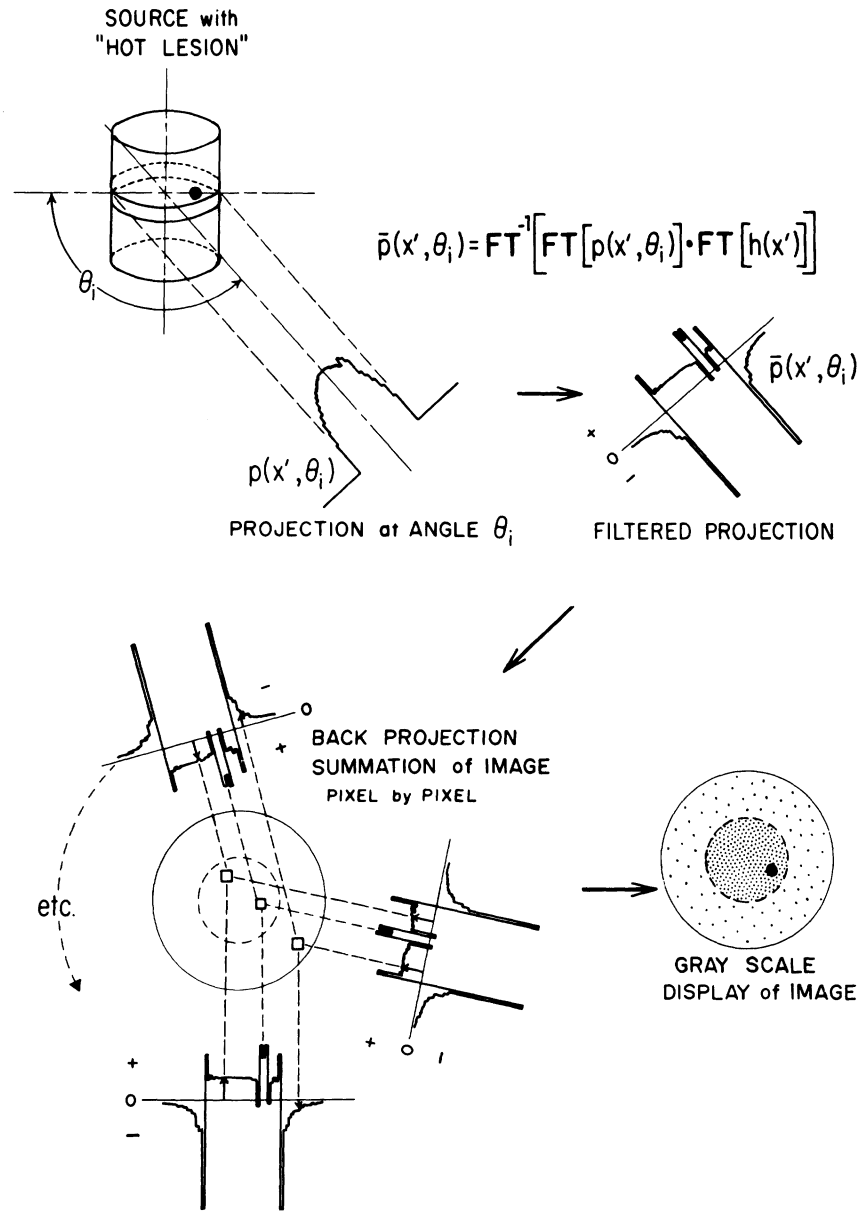


Figure 5. Filtered backprojection reconstruction algorithm. Original projection p is filtered to obtain modified projection $\bar{p}$ (FT indicates Fourier transformation). The reconstructed image is obtained by backprojecting the filtered projections.

Recently several longitudinal section imaging systems have been interfaced to computers and have been used quite successfully for specialized imaging situations. These approaches are described in a later section.

Single photon emission computed tomography (SPECT) is based on the measurement of a set of line integrals or ray sums taken within a section for a complete set of angular samples (Fig. 4). Both scanner based (A) and camera based (B) approaches are used in collecting the projection data of emission densities without interference from overlying and underlying regions of activity.

Transverse section imaging is similar in some respects to transmission or x-ray CT imaging; however, there are several factors unique to SPECT and the reconstruction algorithm must be appropriately modified. In the following sections, these factors are described in more detail together with examples of data processing methods.

## Reconstruction Techniques

Major characteristics of single photon imaging which may affect reconstructed image quality are presented in Table I.

Table I

Factors Affecting Emission Tomographic Image Quality.

1. Backprojection algorithm.
2. Internal gamma ray attenuation.
3. Scattered gamma rays.
4. Limited gamma ray flux.
5. Resolution (collimation variation with depth).
6. Sensitivity errors within the detection system.
7. Angular and spatial sampling.
8. System calibration and alignment.
9. Physiological factors (patient motion, source distribution changes with time, etc.).

It is interesting to note that most of these factors affect not only emission tomographic image quality, but also conventional nuclear medicine imaging. This should not be surprising since conventional projection imaging is simply a case of very incomplete angular sampling, and the backprojection is accomplished by projecting a volume radioactivity distribution onto the detector plane by using a collimator. It appears that dynamic problems such as variations of the source distribution with time (item 9 in Table I) can best be overcome by increasing system sensitivity. However, we have investigated the use of correction algorithms to minimize the effects of patient motion on SPECT image quality.[51]

SPECT Backprojection

There are several review articles[20,45,67,68,69] describing the many possible reconstruction algorithms; thus, a brief summary will only be presented in this manuscript. Basically there are two general classes of solutions used. One class consists of iterative techniques where an initial trial solution is successively modified. The second class is based on a direct analytic reconstruction from the projection data. Presently most x-ray CT and ECT systems use a filtered backprojection technique, which was first proposed by Bracewell and Riddle,[19] and later by Ramachandran and Lakshminarayanan.[23]

The filtered backprojection algorithm used in our camera-based SPECT system[51] is diagramatically shown in Figures 5 and 6. The attenuated Radon transform results in the following expression for the ray sum:

$$p(x_j';\theta_i) = \sum_{k=-\infty}^{\infty} f(x_j', y_k')\exp\left[-\bar{\mu}(x_j', y_k')s(x_j', y_k';\theta_i)\right] \tag{1}$$

where $f(x_j', y_k')$ is the radionuclide source activity at the point $(x_j', y_k')$, $s(x_j', y_k')$ is the distance (path length) from the point $(x_j', y_k')$ to the edge of the body along the ray sum, and $\bar{\mu}(x_j', y_k')$ is the average value of linear attenuation coefficient from the point $(x_j', y_k')$ to the edge of the body along the path length. The rotated and fixed cordinate systems are related by the usual expressions:

$$x' = x\cos\theta_i + y\sin\theta_i \tag{2}$$

$$y' = -x\sin\theta_i + y\cos\theta_i \tag{3}$$

We will defer a discussion of the important aspect of compensating for attenuation in SPECT imaging until the next section. In order to clarify the description of the backprojection process, $\bar{\mu}$ is arbitrarily set equal to zero. In this case the process is equivalent to the transmission CT situation, and an appropriate backprojection algorithm may then be selected from one of the previous cited references.

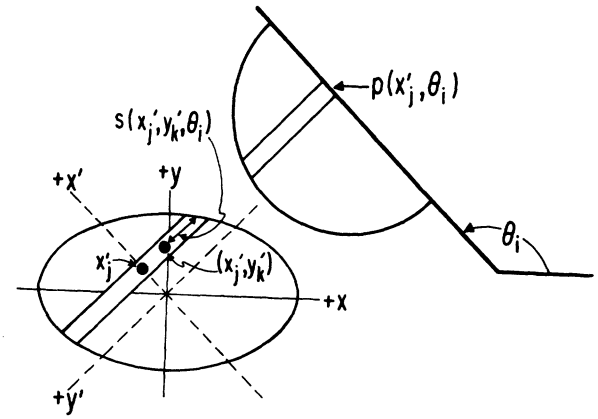


Figure 6. Geometry used to obtain the path length s required for compensation of photon attenuation.

In our SPECT implementation (Fig. 5), we first transform the projections $p(x_j'; \theta_i)$, then multiply by a spatial frequency filter H(f), and finally perform the inverse transform prior to backprojection. In order to more accurately reconstruct the low spatial frequency components, the filter H(f) is generated by computing the Fourier Transform (FT) of the following function:

$$H(f) = FT\{[2f_N\mathrm{sinc}(2f_Nx') - f_N\mathrm{sinc}^2(f_Nx')]\cdot \mathrm{rect}(\frac{x'}{D})\frac{1}{|\Delta x|}\mathrm{comb}(\frac{x'}{\Delta x})\}W(f)\frac{1}{|\Delta f|}\mathrm{comb}(\frac{f}{\Delta f}) \tag{4}$$

D is the diameter of the field of view, $\Delta x$ is the ray sampling interval, $\Delta f$ is the spatial frequency sampling interval, W(f) is an apodization factor, and FT implies Fourier transformation. The functions $\mathrm{rect}(x'/D)$ $\mathrm{comb}(x'/\Delta x)$, $\mathrm{comb}(f/\Delta f)$, $\mathrm{sinc}(2f_Nx')$, $\mathrm{sinc}^2(f_Nx')$ and W(f) are defined by:

$$\mathrm{rect}(\frac{x'}{D}) \triangleq \begin{cases} 1, & |x'| < D/2 \\ \frac{1}{2}, & |x'| = D/2 \\ 0, & |x'| > D/2 \end{cases} \tag{5}$$

$$\frac{1}{|\Delta x|}\mathrm{comb}(\frac{x'}{\Delta x}) \triangleq \sum_{n=-\infty}^{\infty}\delta(x-n\Delta x) \tag{6}$$

$$\frac{1}{|\Delta f|}\mathrm{comb}(\frac{f}{\Delta f}) \triangleq \sum_{n=-\infty}^{\infty}\delta(f-n\Delta f) \tag{7}$$

$$\mathrm{sinc}(2f_Nx') \triangleq \frac{\sin(\pi 2f_Nx')}{\pi 2f_Nx'} \tag{8}$$

$$\mathrm{sinc}^2(f_Nx') \triangleq \frac{\sin^2(\pi f_Nx')}{(\pi f_Nx')^2} \tag{9}$$

$$W(f) \triangleq \frac{1}{2}\left[1 + \cos\left(\frac{\pi|f|}{f_c}\right)\right], |f| \leq f_c$$

$$\triangleq 0 \qquad , |f| > f_c \tag{10}$$

the parameter $f_c$ is the cut off frequency and is usually set equal to some multiple or fractional multiple of the Nyquist or highest sampling frequency $f_N=1/(2\Delta x)$ of the system.[51] The rect function results in a more accurate reconstruction of low spatial frequency, and the window function W(f) provides a convenient method for smoothing in the reconstruction process.

After filtering, the attenuation uncorrected image $f_{unc}(x,y)$ is generated by the conventional backprojection process as shown in Figure 5. Although the above backprojection algorithm (Figs. 5 and 6) schematically illustrates parallel beam geometry, it is possible to also implement fan beam geometry (similar to that of 3rd generation x-ray CT). Our algorithm is based on a Fourier filtering process developed by Jakowatz and Kak[70] and uses specially designed multislice fan beam collimators described previously by Jaszczak et al.[50]

SPECT attenation compensation

The above discussion assumed that the measured ray sum adequately represented the integral of the gamma ray emission density along the ray. The effect of attenuation results in a significant decrease in the measured projection value. Not only is there self-absorption within the organ of interest, but also in the body tissue located between the radionuclide source distribution and the detector. Furthermore, the attenuation coefficient $\mu$ is in general variable for different locations within the body, particularly within the thoracic cavity. Mathematically, the effect of attenuation may be expressed using the exponential or attenuated Radon transform (Eq. 1).

The requirement for an accurate attenuation compensation for "qualitative" SPECT imaging may be of little clinical importance, as has been suggested by Murphy et al.[71] However, if SPECT is to be used to obtain quantitative physiological data, then the effect of attenuation must be carefully considered, and appropriate compensation techniques implemented. (Fig. 7).

Several strategies (of increasing sophistication) have been developed within the last several years. A few possible attenuation compensation approaches have been reviewed by Budinger et al.[45,46,47,60] Most approaches assume a constant value for the attenuation coefficient.

Early techniques used the geometric or arithemtic mean of opposing projections as proposed by Genna[72] and Kay et al[73] respectively. Keyes et al[54] have implemented a SPECT system using the arithmetic mean approach, while Jaszczak et al,[49] Budinger et al[46] and Keyes et al[36] have implemented methods based on the use of the geometric mean.

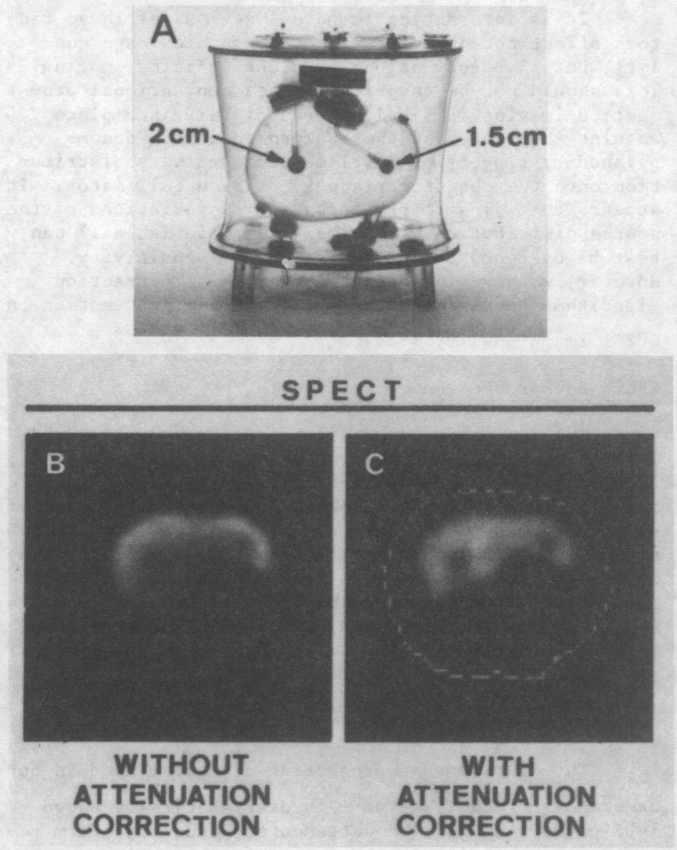


Figure 7. Reconstructed transverse section images of Alderson liver phantom illustrating improvement in image quality obtained from attenation compensation. Data obtained with the Searle-Duke University dual LFOV SPECT system.

Another approach that can generate quantitative SPECT data for certain imaging geometries is based on a normalization of the reconstructed image using data measured from a phantom having known radionuclide concentrations. This technique assumes that the fixed phantom geometry adequately represents the patient geometry. Kuhl et al[33] have implemented this method and have shown that reasonably accurate quantitative results can be obtained when imaging the brain. However, as a result of patient variability, alternative strategies must be used when imaging other parts of the body.

An iterative algorithm based on a convolution technique has been proposed by Walters et al[74] while Hsieh and Wee[75] have proposed an algebraic reconstruction type algorithm to compensate for both attenuation and variations in the point spread response of the detection system. Budinger et al[45,46,47] have described a least squares method which considers the effect of variable attenuation as each iteration is performed; however, all of these approaches currently require significant computation capability in order to be adequately implemented.

As an example of a practical approach our current SPECT system uses the method developed by Chang.[76,77] The method consists of a two-step procedure. A multiplicative correction is used to obtain a first order

corrected image which is then reprojected and compared with the measured projection data to provide a second order correction. The multiplicative correction matrix is defined by (see Fig. 6 and Eq. 1):

$$C_{att}(x_j', y_k') = \frac{f(x_j', y_k')|_{\mu=0}}{f(x_j', y_k')|_{\mu>0}}$$

$$= \frac{1}{\frac{1}{M}\sum_{i=1}^{M} \exp\left[-\mu \cdot s(x_j', y_k'; \theta_i)\right]} \qquad (11)$$

Thus, the correction matrix for a point $(x_j, y_k)$ is related to the average attenuation for that point. The first order corrected image is then given by

$$f_{cor}(x_j', y_k') = f_{unc}(x_j', y_k') C_{att}(x_j', y_k') \qquad (12)$$

Re-projected data are computed using the first order corrected image and a measured body contour. These data are subtracted from the measured projections to generate a set of error projections which are then used to produce an error image. This error image is multiplied by $C_{att}$ and added to $f_{cor}(x,y)$ to obtain the second order corrected image.

It has been found that the first order correction provides an adequate attenuation compensation for most SPECT imaging situations. This method requires that a measurement of the body contour be made. We have developed two techniques for the simultaneous acquisition of body contour data with the acquisition of photopeak projection data.[51] One method uses a Xe-133 transmission line source attached to one LFOV scintillation camera and viewed by the opposing scintillation camera. The second method uses gamma rays which have been Compton scattered within the patient, and thus requires no additional dose to the patient.

Within the last few years the properties of the attenuated Radon transform have been extensively investigated by Tretiak and Delaney[78], Bellini et al[79] and Gullberg.[80] As a result methods of obtaining the convolution filter required to invert the attenuated Radon transform and the limitations on the expected reconstruction accuracy are being defined. However, most practical methods still require a constant or average estimated attenuation coefficient. One method of correcting for non-uniform attenuation would obviously be to first obtain a transmission CT scan to determine the values of the attenuation coefficient.[45] However this requires additional radiation and has some practical difficulties. Recently a new iterative approach based on the analysis of non-linear equations has been proposed by Censor et al[81] that would simultaneoulsy calculate the attenuation coefficients as well as the source activity. It is anticipated that the limitations imposed by nonuniform attenuation will be more precisely determined as newer SPECT systems are developed and used in the clinical environment.

## Gamma ray flux, detection efficiency and collimation

Attenuation compensation can correct the reconstructed image for the observed decrease toward the central portion of the image (Figs. 7 and 10); however, these algorithms can not correct for the loss of statistical image quality resulting from the collection of fewer gamma rays. Thus, in general, reconstructed SPECT images will have more "noise" in the central regions. As a result the statistics will vary from point to point within the image, and an exact theoretical analysis is very difficult. Most investigators have simplified the analysis to predict the signal to noise ratio for specific geometries. For example, Budinger et al[82] have introduced an empirically derived equation applicable to SPECT imaging. Whitehead (private communication) has derived expressions to predict the number of total counts required to detect typical "lesions" in brain and liver phantoms using camera based SPECT systems. This analysis is an extension of a previous investigation of conventional nuclear medicine imaging systems.[83,84]

In any event detection efficiency is important in SPECT imaging. As noted by Keyes[85] and Tretiak[86] SPECT system sensitivity is mainly determined by the "useful" detector area, assuming comparible resolution. In designing SPECT systems it is therefore possible to have high sensitivity for a single slice by concentrating the useful detector area to focus onto a single plane. This approach is often used with scanner based approaches. Conversely camera based SPECT systems view several contiguous slices at one time. Although these multi-slice systems have lower sensitivity per slice, high overall sensitivity is maintained. Keyes[85] has presented a comparison of of useful detector areas of several typical SPECT systems. Besides active detector area, collimation is also important, and it has been shown by Jaszczak et al[50,87] that specially designed collimaton can improve the sensitivity of camera based SPECT systems without loss of spatial resolution in the reconstructed image. Genna et al[88,89] have proposed the use of a curved detector to increase system sensitivity. Lim et al[90] have recently analyzed SPECT system performance for parallel and fan-beam geometries.

The collimation of gamma rays presents some additional mathematical difficulties in SPECT imaging (as did the effects of gamma ray attenuation previously described). The backprojection algorithms assume that the width of each line integral (Fig. 5) is constant and independent of distance from the collimator surface. Unfortunately this assumption is not valid in gamma ray imaging. Since collimators typically consist of a set of channels in a gamma ray absorber such as lead, and since each channel has a specific hole shape, size, and length, the field of view (or solid angle) seen by each individual channel varies with distance from the collimator surface. Cormack[7] in 1973 described this solid angle problem as it relates to the mathematical basis of SPECT. Except for the "half-backprojection" method described by Isenberg and Simon,[91] most SPECT systems do not attempt to compensate for nonuniform depth response by modifying the reconstruction algogorithm. Instead relatively long collimation channels are used in order to minimize rapid variations in solid angle with depth. The uniformity is further improved by collection of projection data for a complete 360° angular scan and using the information contained in opposing views. As a result line spread functions exhibiting reasonable uniformity across the reconstructed image plane have been reported by Budinger et al[45] and Jaszczak et al.[49,51]

## Compton Scattered Gamma Rays

During the collection of SPECT projection data

primary gamma rays are removed either through photoelectric absorption or Compton scattering processes. The latter process is predominant in vivo for gamma ray energies typically used in SPECT imaging. Thus the scattering medium, which includes not only the organ of interest but also surrounding body tissue, behaves essentially as a secondary source of gamma rays whose intensity and energy vary with angle. Whereas attenuation removes signal gamma rays from the ray integral, Compton scattering results in the addition of a systematic background. The magnitude of this background depends not only on sources within the transverse section of interest, but also on sources in other nearby planes.

In theory, scattered gamma rays are of lower energy than the primary gamma rays and could therefore be eliminated by using appropriate energy discrimination techniques. However, most SPECT approaches use NaI(Tl)-photomultiplier detector systems which typically have an energy resolution in the range of 10-15% and require the use of a pulse height window typically corresponding to 10-20% of the mean pulse height of the primary gamma ray energy. These systems then result in the inclusion in the ray sums of photons which have undergone Compton interactions (Fig. 2). One method of minimizing these effects on SPECT imaging would be to use solid state detectors such as high purity Ge which have significantly improved energy resolution. A SPECT system using such detectors is currently being investigated by Ortendahl et al.[92] Practical obstacles include the necessity of cooling the Ge detectors and the high cost of building large area arrays.

The effect of Compton scattering on conventional nuclear medicine imaging has been investigated by Beck et al[93] and Dresser[94]. Recently the effect of single Compton scattering events on SPECT imaging has been investigated by Pang and Genna.[95] Furthermore, a method of compensating for Compton scattering in SPECT imaging based on the use of an integral transport method has been developed by Egbert and May.[96] It is expected that this aspect of SPECT will be more fully investigated within the next several years as quantitative physiological imaging increases in diagnostic importance.

## Angular and Spatial Sampling

Single photon emission computed tomography requires that the section of interest be adequately sampled, both linearly from ray to ray, and angularly from projection set to projection set. The sampling interval requirements for emission CT have recently been reviewed by Phelps.[59]

Even if appropriate algorithms and techniques are used to overcome the physical problems described in the previous sections, it is not possible to obtain artifact free reconstructed images unless the imaging system is carefully designed and built. The following sections describe just a few SPECT design considerations.

Table II lists sampling characteristics of the detector and data processing subsystems which need to be investigated when implementing a single photon emission tomograph. From a theoretical point of view if the object is of finite extent in the spatial domain, then its frequency spectrum is not band limited; thus, suggesting the use of an infinitely small linear sampling interval.

Table II

SPECT Sampling Characteristics

1. The linear sampling interval $\Delta x$ within the section.
2. The angular sampling interval $\Delta\theta$.
3. The spatial frequency sampling interval $\Delta f$.
4. The total number N of linear samples per projection set.
5. The total number M of angular samples per scan.
6. Linear and angular sample to sample sensitivity variations.
7. Differential and integral linearity of the spatial and angular sampling intervals.
8. The linear sampling interval perpendicular to the section.

From a practical point of view the maximum extent of the object is usually determined by the diameter D of the field of view of the detection system; the sampling intervals are then determined by the spatial resolution or the spatial frequency cutoff $f_c$ of the detection system.

The following inequalities can then be derived:

$$\Delta x \leq \frac{1}{2f_c} \tag{13}$$

$$\Delta f \leq \frac{1}{2(D/2)} \tag{14}$$

$$\tan(\Delta\theta) \leq \frac{\Delta x}{(D/2)} = \frac{\Delta f}{f_c} \tag{15}$$

$$M \geq \frac{\pi}{\Delta\theta} \tag{16}$$

$$N \geq \frac{D}{\Delta x} \tag{17}$$

It appears that angular undersampling is less deleterious to SPECT imaging than linear undersampling.[97,98,99] Furthermore, it does not appear to result in significant differences whether the linear and angular samples are acquired with continuous detector motion or with detector indexing ("step and shoot"). Most of the backprojection algorithms previously described assume that the linear and angular sampling intervals are equally spaced. With some SPECT approaches these assumptions are not valid and reconstruction artifacts can result even though the object has been scanned over a complete 360° interval. It should be noted that often $2\pi$, rather than $\pi$, is used in equation (17) for SPECT imaging in order to more adequately compensate for effects of internal gamma ray attenuation and for the effect of solid angle (collimation) variation with depth.

As a result of their limited range of angular view, longitudinal section imaging devices encounter significant mathematical difficulties in attempting to reconstruct artifact free section images of arbitrary source distributions. As a result this manuscript refers to longitudinal tomographic devices as incomplete angular sampling systems, and reserves the term single photon emission computed tomography, or SPECT, to complete angular sampling (transverse section imaging) systems.

Even with complete angular sampling it is possible to have incomplete linear sampling (truncated projections) if the object is larger than the field of view of the gamma ray detecting system (Fig. 8).

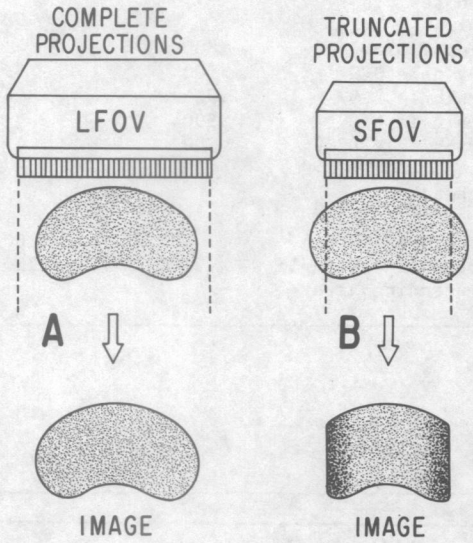


Figure 8. Inadequate field-of-view of detector resulting in truncated projections can generate artifacts in the reconstructed images.

Obviously this problem would be most apparent with camera based approaches; thus, large field of view scintillation cameras are usually preferred, particularly for body imaging. The effects of truncated projections on SPECT image quality has been described by Chang[77] together with some software and hardware compensation techniques.

In addition to the magnitude and number of sampling parameters it is also necessary to consider the effects of regional sensitivity variations. The effect of an increase in sensitivity for the $i^{th}$ ray is illustrated in Figure 9. The error is uniformly large for all projection sets, and thus a uniform circular artifact results. In camera based SPECT systems sensitivity errors may result from energy spectrum variations. They may also result from nonuniform hole-spacing or nonuniform inclusion of foreign material between septa. Although a camera based SPECT system is illustrated in Figure 9, scanner based SPECT systems can also have similar sensitivty errors. These variations are typically corrected by normalizing the detector response to a known source distribution. As shown in Figure 10 this compensation method can significantly improve image quality.

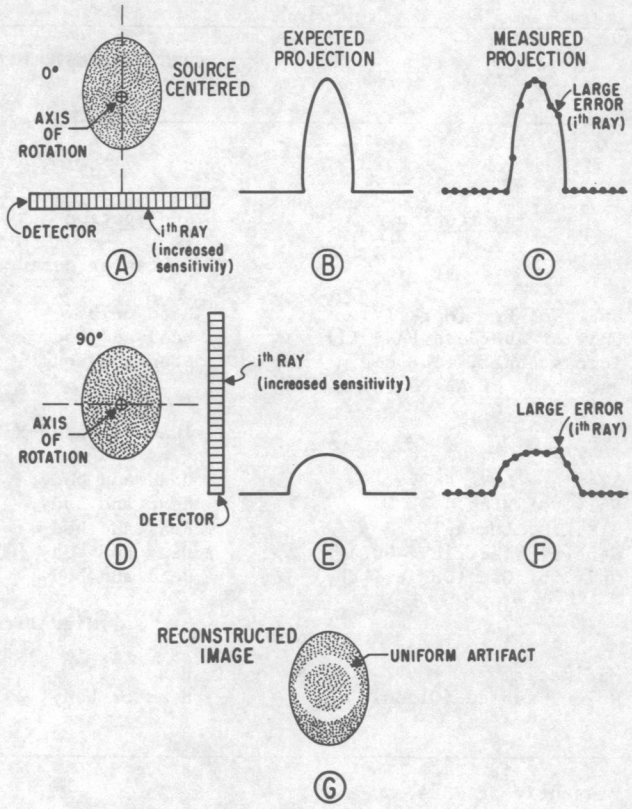


Figure 9. Effect of regional sensitivity variation on reconstructed image quality. Note that error is independent of slope of projection data.

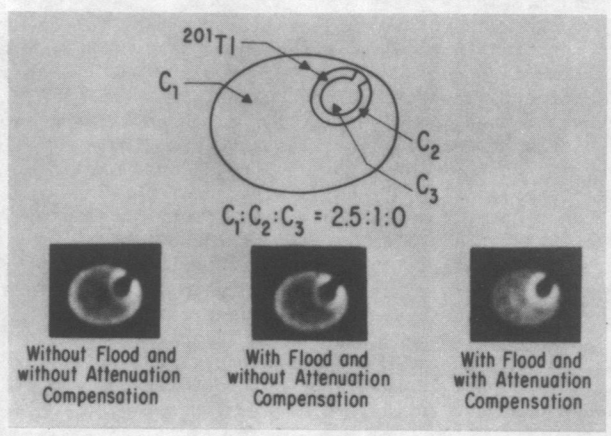


Figure 10. Effect of normalizing projection data to a statically acquired flood source image to compensate for regional sensitivity variations within the scintillation camera. Data obtained with the Searle-Duke University dual LFOV SPECT system.

Careful consideration should also be given to the aspect of spatial distortions, particularly with respect to camera based SPECT systems. Unlike sensitivity errors spatial distortions result in an error which is proportional to the slope of the projection data. It is anticipated that newly developed distortion corrected scintillation cameras will significantly improve SPECT image quality resulting from camera based SPECT systems.

Table III

SPECT---Complete Angular Sampling Systems.

| Institution | Application | Configuration | Estimated Detector area $cm^2$ | [5]References |
|---|---|---|---|---|
| | [Scanner based-single section devices] | | | |
| [1]Univ. of Pa. (Mark IV) | Head only | Square detector array | 608 | 25 - 34 |
| Univ of Aberdeen (ASS II) | Head and body | Square detector array | 1440 | 35 - 37 |
| Tomogscanner, (J&P Engineering and Univ. of Aberdeen) | Head and body | Dual scanner array | 120 | 37 |
| | [Camera based-Multiple section devices] | | | |
| Searle - Duke Univ. | Head and body | Rotating-dual LFOV's | 1800 | 48 - 52 |
| Univ. of Mich. | Head and body | Rotating-single SFOV | 500 | 53 - 54 |
| S.E.L.O. (Milan) | Head and body | Rotating-single LFOV | 900 | 44 |
| [2]General Electric (400T) | Head and body | Rotating-single LFOV | 900 | |
| Univ. of Ca. (Donner Lab.) | Head and body | Stationary-single LFOV | 900 | 45 - 47 |
| | [Miscellaneous approaches] | | | |
| [3]Medimatic | Head only | Square bar-camera array | 985 | 100 |
| [4]Union Carbide (Cleon) | Head or body | Radial-transaxial (single section) scanning array | 3100 | 101 |

[1]Presently at UCLA.
[2]Currently software not supplied for 400T.
[3]Special purpose regional cerebral blow flow system.
[4]Currently not manufactured or marketed.
[5]Numbers refer to those listed at end of manuscript.

Accurate positional amplifier offset voltage calibration is required with camera based SPECT systems in order to obtain high quality SPECT images. The effect of offset voltage misalignment on reconstructed image quality for a source located on the axis of rotation is illustrated in Figure 11. In the top half of the figure the positional amplifier is properly aligned, and an artifact free reconstructed image is obtained. At the bottom of the figure the system is misaligned and the projection data is then peak, for example, in ray 66 instead of between ray 64 and 65. This results in a degraded reconstructed image. Even slight offset voltage misalignment can result in a significant decrease in measured lesion-to-background ratio for small lesions. Hardware or software methods may of course be used to perform this calibration.

SPECT devices using multiple scintillation cameras require additional calibration subsystems (for example, positional amplifier gain adjustments). Design considerations required for camera based (both single and multiple detector heads) have been described by Jaszczak and Coleman.[52]

It is thus apparent from this review that SPECT imaging requires a sophisticated and integrated design approach (including a careful consideration of the interrelationship of software and hardware subsystems) in order to obtain and maintain high quality and artifact free reconstructed images. The following section illustrates a few selected approaches currently being used in emission tomography.

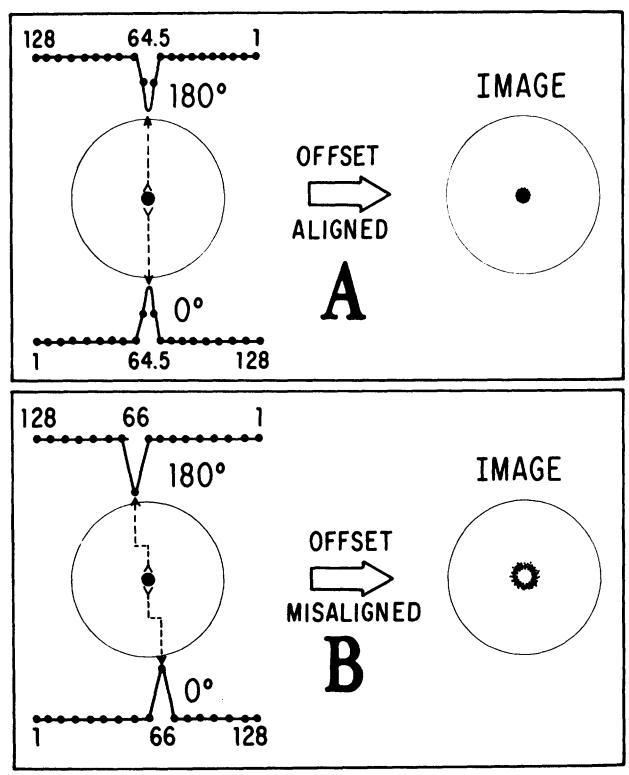


Figure 11. Effect of positional amplifier offset voltage misalignment on reconstructed image quality for a source located on the axis of rotation.

Figure 12.

The Mark IV SPECT system consists of 32 scintillation detectors arranged 8 on a side (courtesy of D. Kuhl).

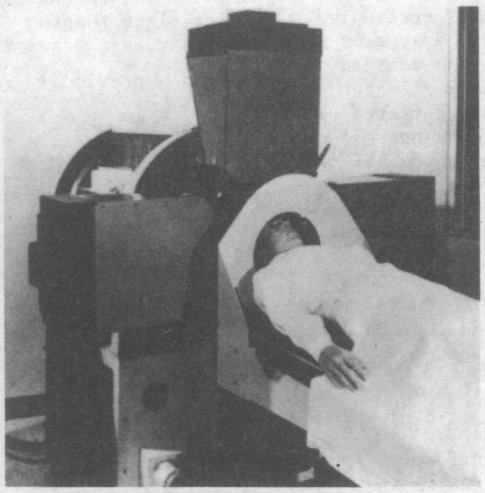

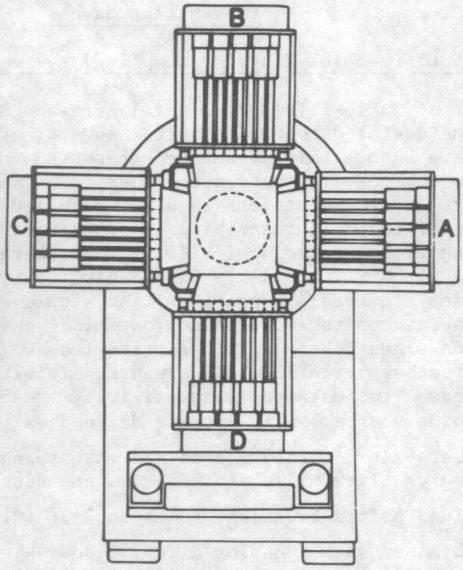


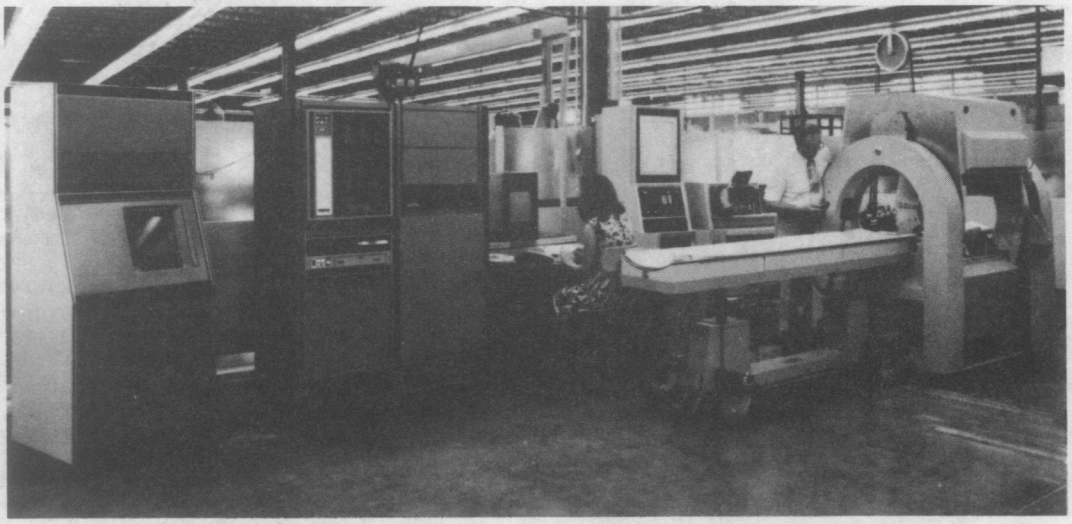

Figure 13.

The Searle-Duke University SPECT system consists of opposed LFOV scintillation cameras mounted in a rotatable gantry.

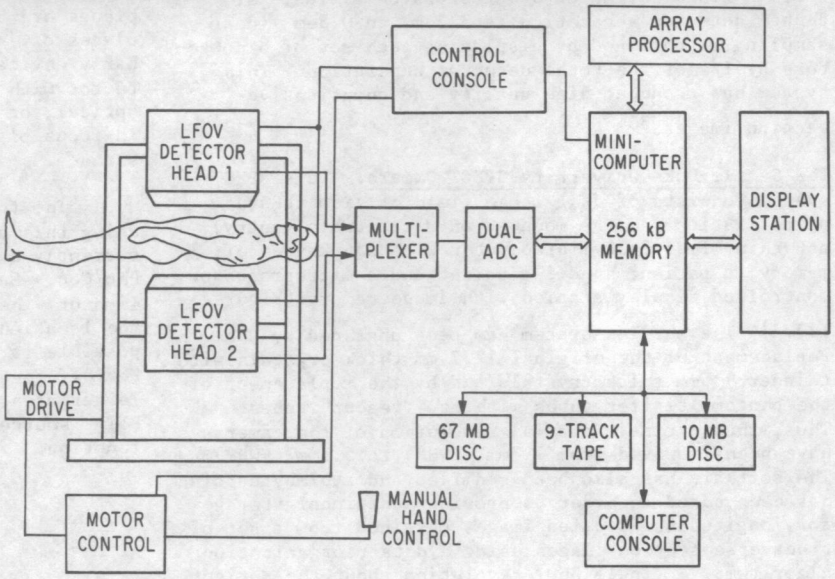

## Current Approaches

### SPECT (complete angular sampling) systems

Table III lists several current SPECT strategies. The useful detector areas for several of the systems have been estimated and are presented in the tables. For the camera based approaches, the useful detector area is somewhat less than the actual detector area. In order to avoid truncation of projection data not all of the circular field of view of the camera can be utilized for SPECT imaging. From Table III two basic strategies are readily apparent. The single section approaches (scanner based) optimize sensitivity within one plane; the multiple section (camera based) approaches optimize whole organ sensitivity. For this reason two measures of sensitivity are often used. The point source sensitivity is defined as the countrate (cnts-sec$^{-1}$ μCi$^{-1}$) obtained when scanning a point source (Tc-99m) in air. The volume sensitivty is defined as the countrate (cnts-sec$^{-1}$)( μCi-cm$^{-3}$)$^{-1}$ obtained when scanning a Tc-99m source uniformly distributed in a long water-filled cylinder 20 cm in diameter. The latter value, although not usually corrected for the inclusion of scattered gamma rays, is a more clinically useful measure. Typical volume sensitivities are 15,400 (cnts-sec$^{-1}$)( μCi-cm$^{-3}$)$^{-1}$ for Mark IV scanner systems[33] and 54,000 (cnts-sec$^{-1}$)( μCi-cm$^{-3}$)$^{-1}$ for the Searle-Duke University camera system.[51] SPECT systems can not be adequately described by sensitivity and resolution since many factors contribute to performance. For example, the Union Carbide scanner[101] has the largest detector area of any system; however, its unique method of data collection results in circularly asymmetric angular sampling which can lead to complications in designing an adequate reconstruction algorithm. Examples of two scanner based and camera based SPECT systems are described below.

The Mark IV. A photograph and a sketch of the Mark IV is shown in Figure 12 and is typical of scanner based SPECT systems.[33] It is appropriate that this system be illustrated first since it evolved from an earlier device developed by Kuhl and Edwards which was the first emission tomographic scanner.[25] The Mark IV consist of 32 NaI(Tl) scintillation crystals (each 7.6 x 2.5 x 2.5cm) arranged 8 detectors on a side. Although detector separation is 3.2cm, an 0.8cm linear sampling is obtained by displacing each set of 8 detectors by 1/4 of the total detector separation. This system has produced high quality and quantitative section images.[33]

The Searle-Duke University SPECT Camera. This SPECT system consists of dual large field of view (LFOV) scintillation cameras mounted on a rotatable gantry, a Perkin-Elmer 8/32 minicomputer with 256 kbytes of memory, a patient handling pallet and a microprocessor controlled display station with image memory (Figure 13).[51] The earlier system has been upgraded by the replacement of the original 12.7 mm thick crystals with thinner 9.5mm thick crystals and by the replacement of the photomultiplier tubes with new "teacup" tubes. Thus, the intrinsic spatial resolution of the cameras have been improved from 7.3mm (FWHM) to 5.1mm (FWHM). The software has also been modified and a 67Mbytes disc has been added in order to provide additional storage for longitudinal section images obtained from a set of transverse section images using a data reorganization algorithm. A single 360° revolution about the patient results in a complete set of 32 transverse, 16 coronal and 16 sagittal section images. An indication of SPECT image quality obtained with a camera based system is shown in the reconstructed transverse section of a Lucite plate phantom (Fig. 14). Experience with earlier camera based SPECT systems developed at Searle have been previously reported.[48,49,71,102]

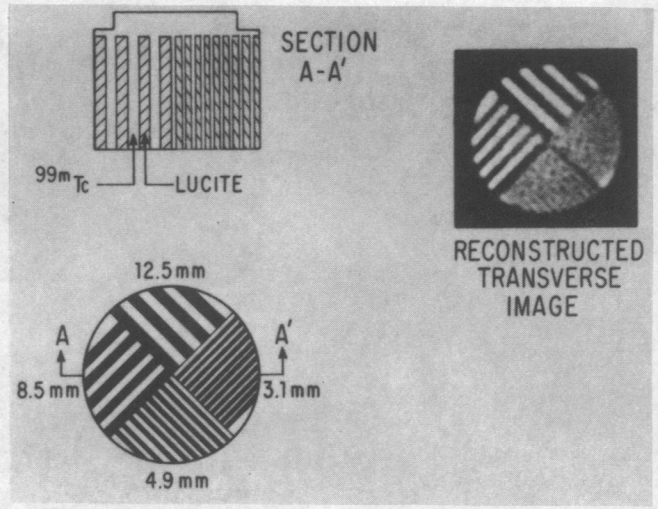


Figure 14. Three-dimensional Lucite plate phantom filled with Tc-99m and imaged with our Searle-Duke University SPECT system. The 4.9mm plates are clearly visible in the reconstructed transverse section image. The slight increase in activity seen within the 3.1mm quadrant results from a physical defect in the phantom.

### Longitudinal (incomplete angular sampling) Systems

Longitudinal section imaging devices are usually based on the focal plane process in which the plane in focus is imaged sharply while the information in other planes are blurred. Usually several longitudinal planes of interest can be generated from a single scan. Early devices combined mechanical motion of the detector with compensation subsystems (either mechanical, optical, or electronic) to generate a discrete set of in-focus planes at fixed distances from the detector surface.

The tomographic scanner developed by Anger[103] using this approach is shown at A in Figure 3, and is currently manufactured by Searle using the brand name Pho/Con. Using the focal length of the converging collimator, the location of the center of the detector and the location of an event on the crystal surface, it is possible to backproject the event onto a set of planes. For off-focal planes these events are spread over a larger area resulting in a lower amplitude background. Point sources thus defocus into a disc-shaped blurring function.

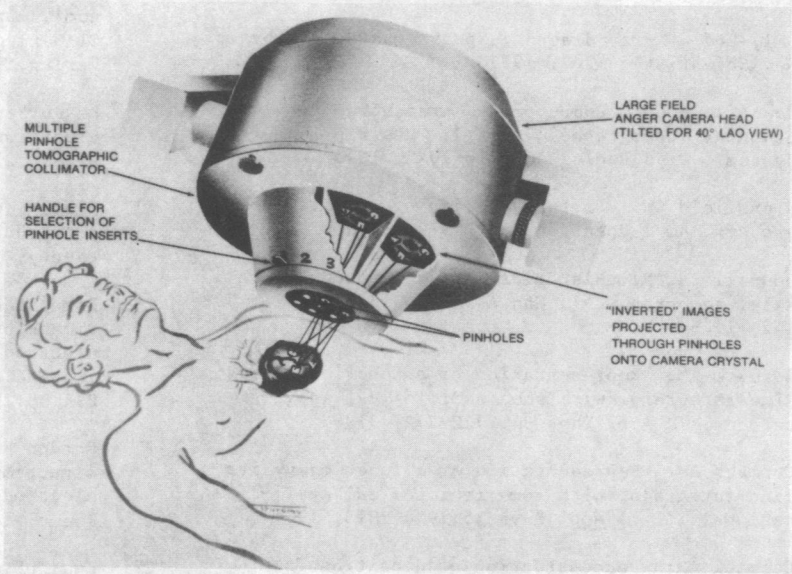


Figure 15. Seven-pinhole emission tomography. By using a an LFOV scintillation camera equipped with a special collimator, it is possible to reconstruct several longitudinal section images of organs such as the heart (courtesy of D.L. Kirch).

Another device in this category is the rotating slant-hole collimator system (Fig. 3-B) developed by Walker,[104] Muehllehner,[105,106] Freedman,[107,108,109] and Cottral and Flioni-Vyza.[110] During a scan the camera is stationary while the slant-hole collimator rotates about an axis of rotation perpendicular to the crystal surface and passing through the center of the crystal. This approach is based on the above described blurring effect, except that in this case a point source defocuses into an annulus rather than a disc. Reconstruction of a discrete set of planes is accomplished by using an electronic circuit to generate a set of compensation voltages synchronized to the motion of the rotating slant-hole collimator.

Recently several of these longitudinal section imaging systems have been interfaced to computers and have been used quite successfully for specialized imaging situations. Nalcioglu et al[111] and Chang et al[112] have interfaced slant-hole collimator systems to digital processing systems and have investigated several reconstruction algorithms. Garcia et al[113] and Pickens et al[114] have interfaced Anger tomographic scanners to minicomputers and attempted to improve sectional image quality by subtracting out of focus information from the planes of interest. These subtraction techniques are all based on the method originally developed by Chang et al[115] to improve tomographic image quality obtained from a set of pinholes sequentially veiwing a source distribution from different directions.

One approach that has generated considerable interest recently is the 7-pinhole system developed by Vogel[116] and is illustrated in Figure 15. This approach uses a nonlinear reconstruction algorithm to generate a set of longitudinal cardiac sections. This technique is somewhat analagous to emission coded aperture imaging which was first developed by Barrett[117] and has subsequently been investigated by several groups (for example, see Rogers et al,[118] Jaszczak et al,[119] Williams et al[120] and Renaud et al.[121]) However, in the 7-pinhole system overlap of data from the multiple pinholes is eliminated by internal septa; thus, simplifying the reconstruction problem. Presently all of the above approaches do not provide complete angular sampling and have been clinically most useful in imaging relatively small organs such as the heart which have a larger proportion of high spatial frequencies relative to low spatial frequencies. These approaches do have the advantage of being inexpensive to implement and may provide valuable information in carefully selected clinical situations.

## Conclusions

Much progress has been made during the last several years in developing new techniques and improving the quality of both transverse section and longitudinal section single photon tomographs. The recent availability of high quality SPECT systems has led to a renewed interest in single photon radiopharmaceutical development directed specifically toward the utilization of these devices. For example, Kung and Blau recently proposed a new mechanism for uptake in the brain based on pH gradients within the body and on the lipid-solubility of certain compounds.[122] Initial results indicate that the regional distribution of these compounds is similar to that of deoxyglucose and thus may be useful in describing brain metabolism. It is anticipated that development in single photon radiopharmaceutical will result in increased interest in using SPECT systems to make quantitative measurements of important physiological processes.

## Acknowledgements

We wish to acknowledge valuable discussions with several investigators in the area of single photon emission tomography. We wish to particularly acknowledge those scientists who supplied useful and complete information. We are also grateful to Rose Boyd for her excellent secretarial support in preparing this manuscript.

## References


1. EMI, Ltd: X-ray diagnosis peers inside the brain. New Scientist 54:207, 1972

2. Hounsfield GN: Computerized transverse axial scanning (tomography): Part 1. Description of system. Br J Radiol 46:1016-1022, 1973

3. Hounsfield GN: Picture quality of computed tomography. Am J Roentgenol 127:3-9, 1976

4. Hounsfield GN: Historical notes on computerized axial tomography. J Can Assoc Radiolgists 27:135-142, 1976

5. Cormack AM: Representation of a function by its line integrals, with some radiological applications. J Appl Phys 34:2722-2727, 1963

6. Cormack AM: Representation of a function by its line integrals, with some radiological applications. II J Appl Phys 35:2908-2913, 1964

7. Cormack AM: Reconstruction of densities from their projections, with applications in radiological physics. Phys Med Biol 18:195-207, 1973

8. Oldendorf WH: Isolated flying spot detection of radiodensity discontinuities--Displaying the internal structural pattern of a complex object. IRE Trans Bio-Med Electronics BME-8:68-72, 1961

9. Berry MV, Gibbs DF: The interpretation of optical projections. Proc Roy Soc Lond A 314:143-152, 1970

10. Shepp LA, Logan BF: Reconstructing interior head tissue from x-ray transmissions. IEEE Trans Nucl Sci NS-21:228-236, February, 1974

11. Herman GT, Lakshminarayanan AV, and Naparstek A: Reconstruction using divergent-ray shadowgraph. In Reconstruction Tomography in Diagnostic Radiology and Nuclear Medicine, Ed. MM Ter-Pogossian, et al (Baltimore: University Park Press, 1977) pp 105-117

12. Bates RHT, Peters TM: Towards improvements in tomography. New Zealand J Sci 14:883-896, 1971

13. Smith PR, Peters TM, Bates RHT: Image reconstruction from finite numbers of projections. J Phys A: Math, Nucl Gen 6:361-382, 1973

14. Peters TM, Smith PR, Gibson RD: Computer aided transverse body-section radiography. Br J Radiol 46:314-317, 1973

15. Goitein M: Three-dimensional density reconstruction from a series of two-dimensional projections. Nucl Instrum Methods 101:509-518, 1972

16. Radon J: Uber die bestimmung von funktionen durch ihre integralwerte langs gewisser mannigfaltigkeiten. Ber Verh Sachs Akad Wiss 67: 262-277, 1917

17. Bracewell RN, Roberts JA: Aerial smoothing in radio astronomy. Aust J Phys 7:615-640, 1954

18. Bracewell RN: Strip integration in radio astronomy. Aust J Phys 9:198-217, 1956

19. Bracewell RN, Riddle AC: Inversion of fan-beam scans in radio astronomy. Astrophys J 150:427-434, 1967

20. Bracewell RN: Image restoration in radio astronomy. In Topics in Applied Physics, Vol 32. Ed GT Herman (Berlin Heidelberg New York: Springer-Verlag, 1979) pp 81-104

21. De Rosier DJ, Klug A: Reconstruction of three dimensional structures from electron micrographs. Nature 217:130-134, 1968

22. Klug A, Crowther RA: Three-dimensional image reconstruction from the viewpoint of information theory. Nature 238:435-440, 1972

23. Ramachandran GN, Lakshminarayanan AV: Three dimensional reconstruction from radiographs and electron micrographs: Application of convolutions instead of Fourier transforms. Proc Nat Acad Sci USA 68:2236-2240, 1971

24. Gordon R, Bender R, Herman GT: Algebraic reconstruction techniques (ART) for three-dimensional electron microscopy and x-ray photography. J Theor Biol 29:471-481, 1970

25. Kuhl DE, Edwards RQ: Image separation radioisotope scanning. Radiology 80:653-662, 1963

26. Kuhl DE, Edwards RQ: Cylindrical and section radioisotope scanning of the liver and brain. Radiology 83:926-935, 1964

27. Kuhl DE, Edwards RQ: Reorganizing data from transverse section scans of the brain using digital processing. Radiology 91:975-983, 1968

28. Kuhl DE: The current status of tomographic scanning. In Fundamental Problems in Scanning. Ed A Gottschalk, RN Beck (Springfield, IL: Charles C Thomas, 1968) pp 179-190

29. Kuhl DE, Edwards RQ: The Mark III scanner: A compact device for multiple-view and section scanning of the brain. Radiology 96:563-570, 1970

30. Kuhl DE, Edwards RQ, Ricci AR, Reivich M: Quantitative section scanning using orthogonal tangent correction. J Nucl Med 14:196-200, 1973

31. Kuhl DE, Edwards RQ, Ricci AR, Reivich M: Quantitative section scanning. In Medical Radioisotope Scintigraphy 1972, Vol I (Vienna: International Atomic Energy Agency, 1973) pp 347-353

32. Kuhl DE, Edwards RQ, Ricci AR: Transverse section scanner at the University of Pennsylvania In Tomographic Imaging in Nuclear Medicine, Ed GS Freedman (New York: Society Nuclear Medicine, 1974) pp 19-27

33. Kuhl DE, Edwards RQ, Ricci AR, Yacob RJ, Mich TJ, Alavi A: The Mark IV system for radionuclide computed tomography of the brain. Radiology 121:405-413, 1976

34. Kuhl DE, Hale J, Eaton WL: Transmission scanning: A useful adjunct to conventional emission scanning for accurately keying isotope deposition to radiographic anatomy. Radiology 87:278-284, 1966

35. Bowley AR, Taylor CG, Causer DA, Barber DC, Keyes WI, Undrill PE, Corfield JR, Mallard JR: A radioisotope scanner for rectilinear, arc, transverse section and longitudinal section scanning: (ASS--the Aberdeen Section Scanner). Br J Radiol 46: 262-271, 1973

36. Keyes WI: A practical approach to transverse-section gamma-ray imaging. Br J Radiol 49:62-70, 1976

37. Myers MJ, Keyes WI, Mallard JR: An analysis of tomographic scanning systems. In Medical Radioisotope Scintigraphy 1972 Vol I (Vienna: International Atomic Energy Agency, 1973) pp 331-346

38. Patton JA, Brill AB, King PH: A new mode of collection and display of three-dimensional data for static and dynamic radiotracer studies. In Radioisotope Scintigraphy 1972, Vol I (Vienna: International Atomic Energy Agency, 1973) pp 355-368

39. Patton JA, Brill AB, King PH: Transverse section brain scanning with a multicrystal cylindrical imaging device. In Tomographic Imaging In Nuclear Medicine, Ed GS Freedman (New York: Society of Nuclear Medicine, 1973) pp 28-43

40. Anger HO, Price DC, Yost PE: Transverse-section tomography with the scintillation camera. J Nucl Med 8:314-315, 1967

41. Anger HO: The scinitllation camera for radioisotope localization. In Radioisotope in der Lokalisationsdiagnostik Nucl Med Suppl 6, Ed G Hoffman, KE Scheer (Stuggart: Schattauer-Verlag, 1967) pp 1-21

42. Harper PV, Beck RN, Charleston DE, Brunsden B, Lathrop KA: The three dimensional mapping and display of radioisotope distributions. J Nucl Med 6:332, 1965

43. Harper PV: The three-dimensional reconstruction of isotope distributions. In Fundamental Problems in Scanning. Ed. A Gottschalk, RN Beck (Springfield, Il: Charles C Thomas, 1968) pp 191-194

44. Bellini S, Piacentini M, Cafforio C, Rocca F: Design of a computerized emission tomographic system. Signal Processing 1:125-131, 1979

45. Budinger TF, Gullberg GT: Three-dimensional reconstruction in nuclear medicine emission imaging. IEEE Trans Nucl Sci NS-21:2-20, June, 1974

46. Budinger TF, Derenzo SE, Gullberg GT, Greenberg WL, Heusman RH: Emission computer assisted tomography with single-photon and positron annihilation photon emitters. J Comput Assist Tomog 1: 131-145, 1977

47. Budinger TF, Gullberg GT: Transverse section reconstruction of gamma-ray emitting radionuclides in patients. In Reconstruction Tomography in Diagnostic Radiology and Nuclear Medicine. Ed MM Ter-Pogossian, et al (Baltimore University Park Press, 1977) pp 315-342

48. Jaszczak R, Huard D, Murphy P, Burdine J: Radionuclide emission computed tomography with a scintillation camera. J Nucl Med 17:551, 1976

49. Jaszczak RJ, Murphy PH, Huard D, Burdine JA: Radionuclide emission computed tomography of the head with $^{99m}$Tc and a scintillation camera. J Nucl Med 18:373-380, 1977

50. Jaszczak RJ, Chang LT, Murphy PH: Single photon emission computed tomography using multi-slice fan beam collimators. IEEE Trans Nucl Sci NS-26, 610-618, 1979

51. Jaszczak RJ, Chang LT, Stein NA, Moore FE: Whole-body single-photon emission computed tomography using dual, large-field-of-view scintillation cameras. Phys Med Biol 24:1123-1143, 1979

52. Jaszczak RJ, Coleman RE: Selected processing techniques for scintillation camera based SPECT systems. In Procedings of Tenth Symposium on the Sharing of Computer Programs and Technology in Nuclear Medicine. (New York: Society of Nuclear Medicine, 1979) in press

53. Kay DB, Keyes Jr JW, Simon W: Radionuclide tomographic image reconstruction using Fourier transform techniques. J Nucl Med 15:981-986, 1974

54. Keyes Jr JW, Orlandea N, Heetderks WJ, Leonard PF, Rogers WL: The humogotron--A scintillation-camera transaxial tomography. J Nucl Med 18:381-387, 1977

55. Oppenheim BE: More accurate algorithms for iterative 3-dimensional reconstruction. IEEE Trans Nucl Sci NS-21, 72-77, June, 1974

56. Oppenheim BE, Hoffer PB, Gottschalk A: Nuclear imaging: A new dimension. Radiology 118:491-494, 1976

57. Muehllehner G: Radioisotope imaging in three dimensions. J Nucl Med 9:337, 1968

58. Muehllehner G, Wetzel RA: Section imaging by computer calculation. J Nucl Med 12:76-84, 1971

59. Phelps ME: Emission computed tomography. Semin Nucl Med 7:337-365, 1977

60. Budinger TF, Gullberg GT, Huesman RH: Emission computed tomography. In Topics in Applied Physics Vol 32. Ed GT Herman (Berlin Heidelberg New York Springer-Verlag, 1979) pp 147-246

61. Cassen B, Curtis L, Reed CW: A sensitive directional gamma-ray detector. Nucleonics:78-81, February, 1950

62. Cassen B, Curtis L, Reed C, Libby R: Instrumentation for $I^{131}$ use in medical studies. Nucleonics: 46-50, August, 1951

63. Anger HO: Scintillation camera. Rev Sci Instrum 29:27-33, 1958

64. Anger HO: Scintillation camera with multichannel collimators. J Nucl Med 5:515-531, 1964

65. Harper PV, Andros G, Lathrop K, Siemens W, Weiss L: Technetium-90, as a biological tracer. J Nucl Med 3:209, 1962

66. Harper PV, Lathrop KA, Jiminez F, Fink R, Gottschalk A: Technetium 99m as a scanning agent. Radiology 85 101-109, 1965

67. Gordon R: A tutorial on ART (Algebraic reconstruction techniques). IEEE Trans Nucl Sci NS-21, 78-93, June, 1974

68. Brooks RA, Di Chiro G: Theory of image reconstruction in computed tomography. Radiology 117: 561-572, 1975

69. Brooks RA, Di Chiro G: Principles of computer assisted tomography (CAT) in radiographic and radioisotopic imaging. Phys Med Biol 21:689-732, 1976

70. Jakowatz CV, Kak AC: Computerized tomographic imaging using x-rays and ultrasound. TR-EE 76-26 (Purdue University, July, 1976)

71. Murphy PM, Thompson WL, Moore ML, Burdine JA: Radionuclide computed tomography of the body using routine radiopharmaceuticals. I. System characterization. J Nucl Med 20:102-107, 1979

72. Genna S: Analytical methods in whole-body counting. In Clinical Uses of Whole-Body Counting (Vienna: International Atomic Energy Agency, 1966) pp 37-63

73. Kay DB, Keyes Jr JW: First order corrections for absorbtion and resolution compensation in radionuclide Fourier tomography. J Nucl Med 16:540-541, 1975

74. Walters TE, Simon W, Chesler DA, Correia JA, Riederer SJ: Radionuclide axial tomography with correction for internal absorption. In Information Processing in Scintigraphy, Procedings of the IVth International Conference (Orsay, 1975) pp 333-342

75. Hsieh RC, Wee WG: On methods of three-dimensional reconstruction from a set of radioisotope scintigrams. IEEE Trans on Systems, Man and Cybernetics SMC-6:854, 1976

76. Chang, LT: A method for attenuation correction in radionuclide computed tomography. IEEE Trans Nucl Sci NS-25:638-642, 1978

77. Chang LT: Attenuation correction and incomplete projection in single photon emission computed tomography. IEEE Trans Nucl Sci NS-26:2780-2789, 1978

78. Tretiak OJ, Delaney P: The exponential convolution algorithm for emission computed axial tomography. In Information Processing in Medical Imaging (Nashville: Biomedical Computing Technology Information Center, 1977) pp 266-289

79. Bellini S, Piacentini M, Cafforio C, Rocca F: Compensation of tissue absorption in emission tomography. IEEE Trans Acoustics, Speech Signal Processing ASSP-27:213-218, 1979

80. Gullberg GT: The attenuated Radon transform: Theory and application in medicine and biology. PhD thesis (Berkeley: University of California, June, 1979)

81. Censor Y, Gustafson DE, Lent A, Tuy H: A new approach to the emission computerized tomography problem: Simultaneous calculation of attenuation and activity coefficients. In press.

82. Budinger TF, Cahoon JL, Derenzo SE, Gullberg GT, Moyer BR, Yano Y: Three dimensional imaging of the myocardium with radionuclides. Radiology 125: 433-439, 1977

83. Whitehead FR: Quantitative analysis of minimum detectable lesion-to-background uptake ratios for nuclear medicine imaging systems. In Medical Radionuclide Imaging Vol I. (Vienna: International Atomic Energy Agency, 1977) pp 409-434

84. Whitehead FR: Minimum detectable gray-scale differences in nuclear medicine images. J Nucl Med 19:87-93, 1978

85. Keyes WI: Current status of single photon emission computerized tomography. IEEE Trans Nucl Sci NS-26:2752-2755, 1979

86. Tretiak OJ: Fundamental limitations in radionuclide imaging. In Computer Aided Tomography and Ultrasonics in Medicine. Ed. Raviv, et al (North Holland Publishing Company, 1979) pp 109-122

87. Jaszczak RJ: Collimator trans-axial tomographic scintillation camera. United States Patent Number 4057726, 1977

88. Genna S, Pang SC, Burrows BA: Analysis of an arcuate gamma camera design for transaxial reconstruction. In Medical Radionuclide Imaging Vol I (Vienna: International Atomic Energy Agency 1977) pp 323-339

89. Genna S, Pang SC, Burrows BA: Application of fan reconstruction geometries to transmission and emission systems. In Reconstruction Tomography in Diagnostic Radiology and Nuclear Medicine. Ed. MM Ter-Pogossian, et al (Baltimore: University Park Press, 1977) pp 139-154

90. Lim CB, Chang LT, Jaszczak RJ: Performance analysis of three camera configurations for single photon emission computed tomography. IEEE Trans Nucl Sci NS-27: in press

91. Isenberg JF, Simon W: Radionuclide axial tomography by half back-projection. Phys Med Biol 23:154-158, 1978

92. Ortendahl D, Kaufman L, Watts J: High resolution single-photon emission computed tomography with a small germanium camera. IEEE Trans Nucl Sci NS-27: in press

93. Beck RN, Schuh MW, Cohen TD, Lembares N: Effects of scattered radiation on scintillation detector response. In Medical Radioisotope Scintigraphy Vol I (Vienna: International Atomic Energy Agency, 1969) pp 595-616

94. Dresser MM, Knoll GF: Results of scattering in radioisotope imaging. IEEE Trans Nucl Sci NS-20: 266-272, 1973

95. Pang SC, Genna S: The effect of Compton scattered photons on emission computerized transaxial tomography. IEEE Trans Nucl Sci NS-26:2771-2774, 1979

96. Egbert SD, May RS: An integral-transport method for Compton-scatter correction in emissiom computed tomography. IEEE Trans Nucl Sci NS-27: in press, 1980

97. Shepp LA, Stein JA: Simulated reconstruction artifacts in computerized x-ray tomography. In Reconstruction Tomography in Diagnostic Radiology and Nuclear Medicine. Ed. MM Ter-Pogossian, et al (Baltimore: University Park Press, 1977) pp 33-48

98. Crawford CR and Kak AC: Aliasing artifacts in computerized tomography. Appl Optics 18:3704-3711, 1979

99. Brooks RA, Weiss GH, Talbert AJ: A new approach to interpolation in computed tomography. J Comput Assist Tomog 2:577-585, 1978

100. Lassen NA, Sveinsdottir E, Kanno I, Stokely EM, Rommer P: A fast moving single photon emission tomograph for regional cerebral blood flow studies in man. J Comput Assist Tomog 2:661-662, 1978

101. Stoddart HF, Stoddart HA: A new development in single gamma transaxial tomography Union Carbide focused collimator scanner. IEEE Trans Nucl Sci NS-26:2710-2712, 1979

102. Burdine JA, Murphy PH, DePuey EG: Radionuclide computed tomography of the body using routine radiopharmaceuticals. II. Clinical applications. J Nucl Med 20:108-114, 1979

103. Anger HO: Multiplane tomographic gamma-ray scanner. In Medical Radioisotope Scintigraphy Vol I. (Vienna: International Atomic Energy Agency, 1969) pp 203-216

104. Walker WG: Tomographic radiation camera. United States Patent Number 3612865

105. Muehllehner G: Rotating collimator tomography. J Nucl Med 11:347, 1970

106. Muehllehner G: Performance parameters for a tomographic scintillation camera. In Tomographic Imaging in Nuclear Medicine. Ed. GS Freedman (New York: Society of Nuclear Medicine, 1973) pp 76-83

107. Freedman GS: Tomography using a scintillation camera, a digital computer and a special collimator. J Nucl Med 11:319-320, 1970

108. Greedman GS: Tomography with a gamma camera. J Nucl Med 11:602-604, 1970

109. Freedman GS: Digital gamma camera tomography--theory. In Tomographic Imaging in Nuclear Medicine. Ed. GS Freedman (New York: Society of Nuclear Medicine, 1973) pp 68-75

110. Cottrall MF, Flioni-Vyza A: Design of a scintillation camera tomographic system and investigations of its performance. In Medical Radioisotope Scintigraphy 1972. (Vienna: International Atomic Energy Agency, 1973) pp 381-408

111. Nalcioglu O, Morton ME: Computerized longitudinal tomography (CLT) with a bilateral collimator. IEEE Trans Nucl Sci NS-27: in press, 1980

112. Chang W, Lin SL, Salo, BC, Henkin RE: 4-quadrant rotating slant hole collimator for limited angle computerized tomography. In Procedings of Tenth Symposium on Computer Programs and Technology in Nuclear Medicine (Miami Beach: Society of Nuclear Medicine, 1980) in press

113. Garcia E, Diaz J, Chapman D, Berman D, Waxman A: Single photon emission computed tomography using a multiplane scanner. IEEE Trans Nucl Sci NS-27: in press, 1980

114. Pickens DR, Price RR, Patton JA, Erickson JJ, Rollo FD, Brill AB: Focal-plane tomography image reconstruction. IEEE Trans Nucl Sci NS-27: in press, 1980

115. Chang LT, Macdonald B, Perez-Mendez V: Axial tomography and three dimensional image reconstruction. IEEE Trans Nucl Sci NS-23:568-572, 1976

116. Vogel RA: A new method of multiplaner emission tomography using a seven pinhole collimator and an Anger camera. J Nucl Med 19:648-654, 1978

117. Barrett HH: Fresnel zone plate imaging in nuclear medicine. J Nucl Med 13:382-385, 1972

118. Rogers WL, Han KS, Jones LW, Beierwalters WA: Application of a fresnel zone plate to gamma-ray imaging. J Nucl Med 13:612-615, 1972

119. Jaszczak RJ, Moore FE, Whitehead FR: Use of an array of three off-axis zone plates for large field of view gamma ray imaging. In Application of Optical Instrumentation in Medicine-II. Ed WR Hendee, WC Zarnsorff (Palos Verdes Estates, California: Society of Photo-optical Instrumentation Engineers, 1974) pp 3-9

120. Williams JJ, Knoll GF: Initial performance of SPRINT: A single photon system for emission tomography. IEEE Trans Nucl Sci NS-26;2732-2735, 1979

121. Renaud L, Joy MLG, Gilday D: Fourier multiperture emission tomography (FMET). IEEE Trans Nucl Sci NS-27: in press, 1980

122. Kung HF, Blau M: Regional intracellular pH shift: A proposed new mechanism for radiopharmaceutical uptake in brain and other tissues. J Nucl Med 21:147-152, 1980